Structure and mechanism of an intramembrane liponucleotide synthetase central for phospholipid biosynthesis

Xiuying Liu[1,3], Yan Yin[1,2,3], Jinjun Wu[1] and Zhenfeng Liu[1]

[1]*National Laboratory of Biomacromolecules, Institute of Biophysics, Chinese Academy of Sciences, 15 Datun Road, Chaoyang District, Beijing, People's Republic of China.* [2]*University of Chinese Academy of Sciences, Beijing, People's Republic of China.*

[3]These authors contributed equally to the project.

Supplementary Figures 1-10 and Table 1.

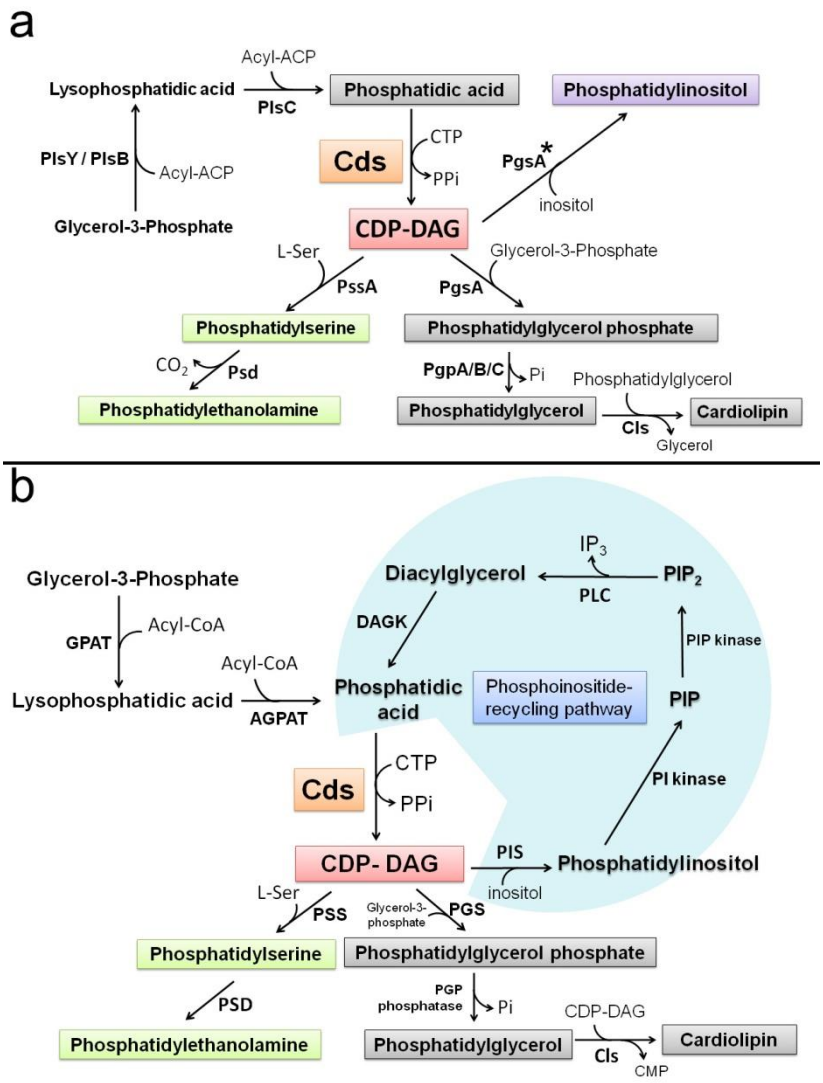

Supplementary Figure 1 | The CDP-DAG mediated phospholipid biosynthesis and recycling pathways in prokaryotic and eukaryotic organisms. (a) Prokaryotic phospholipid biosynthesis pathways mediated by CDP-DAG. ACP, acyl carrier protein; PlsY/PlsB, Glycerol-3-phosphate acyltransferase; PlsC, 1-acyl-sn-glycerol-3-phosphate acyltransferase; Cds: CDP-DAG synthetase, encoded *CdsA* gene in prokaryotes (or by *CDS* genes in eukaryotes). PssA, bacterial phosphatidylserine synthase; Psd, phosphatidylserine decarboxylase; PgsA, phosphatidylglycerol phosphate (PGP) synthase; PgsA***,** The *pgsA* gene in *M. smegmatis* encodes the phosphatidylinositol synthase enzyme. PgpA/B/C, PGP phosphatases; Cls, cardiolipin synthase. **(b)** Eukaryotic phospholipid biosynthesis and

recycling pathways mediated by CDP-DAG. GPAT, Glycerol-3-phosphate acyltransferase; AGPAT, 1-acylglycerol-3-phosphate-O-acyltransferase; PI kinase, phosphatidylinositol kinase; PIP kinase, phosphatidylinositol phosphate kinase; PLC, phospholipase C; DAGK, diacylglycerol kinase; PGS, PGP synthase; PSS, phosphatidylserine synthase found in *Saccharomyces cerevisiae* and some plants (such as wheat) with function similar to that of bacterial PssA; PSD, phosphatidylserine decarboxylase.

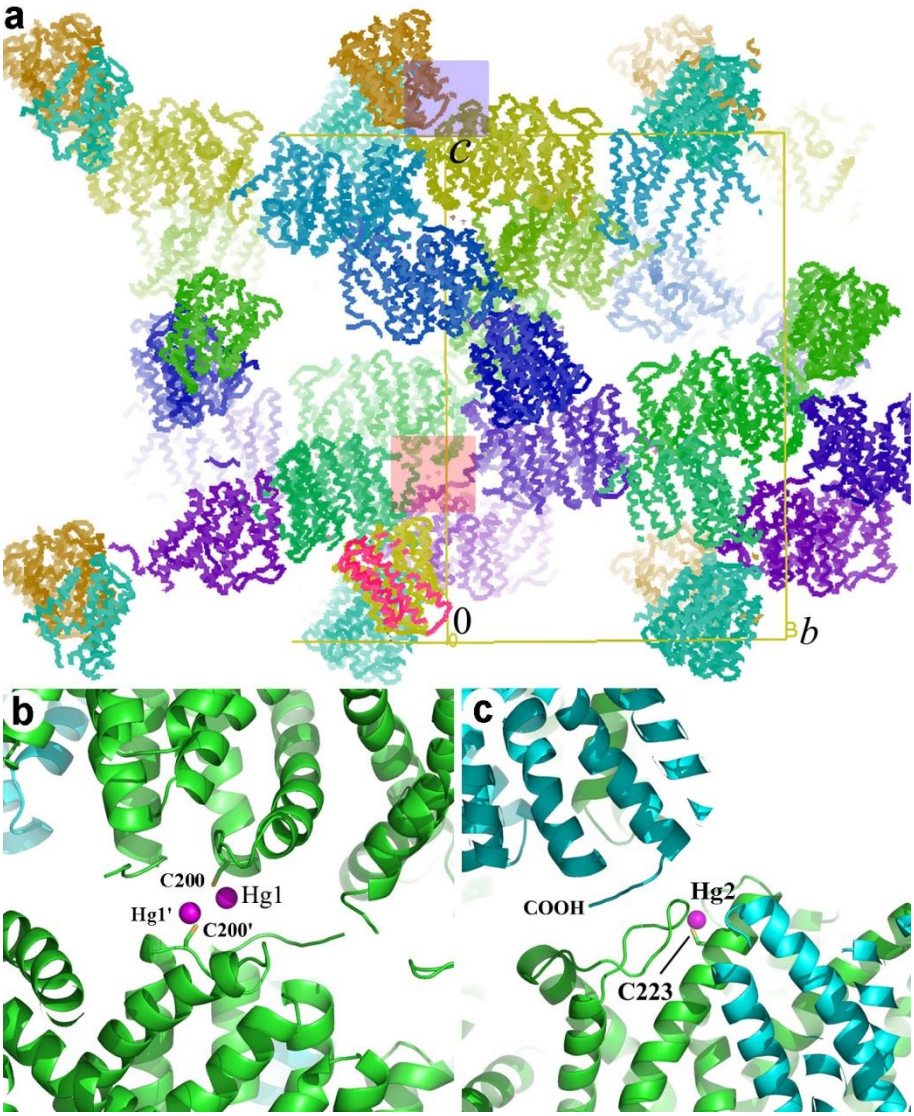

Supplementary Figure 2 | Role of methylmercury in stabilizing the crystal packing interfaces between adjacent TmCdsA molecules. (**a**) Overview of the crystal packing of TmCdsA. (**b** and **c**) Zoom-in views of the red (b) and blue-box (c) shaded interfacial regions shown in a**,** respectively. Mercury atoms are shown as purple spheres and the cysteine residues involved in binding methylmercury groups are presented as stick models.

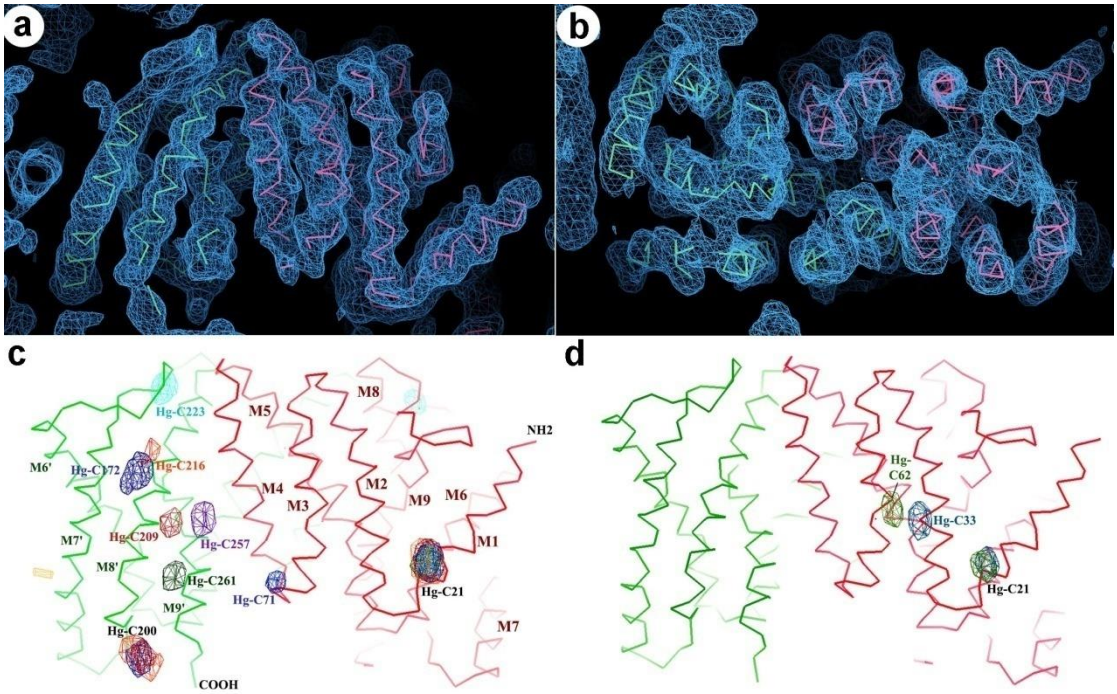

Supplementary Figure 3 | The experimental electron density maps of TmCdsA. **(a, b)** The initial electron density map at 3.8 Å resolution output by the Phenix Autosol program with Autobuild model superposed on the map. The map is viewed along the membrane plane (a) or along the membrane normal from periplasmic side (b). **(c, d)** Anomalous difference Fourier maps of various mercury derivatives used as site-specific labels for the verification of sequence registration during structural model building and refinement.

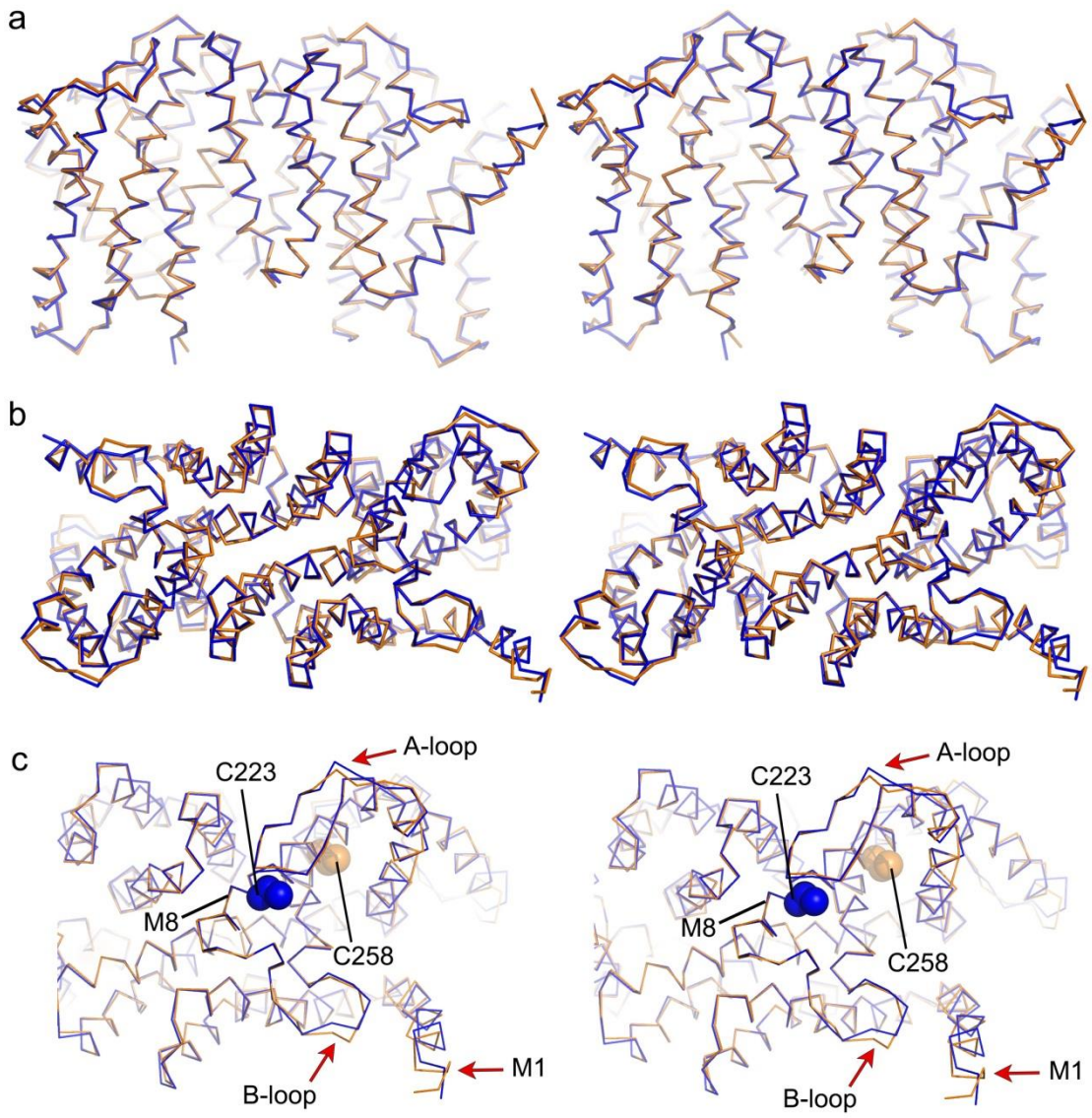

Supplementary Figure 4 | Superposition of the overall structures of S200C/S223C (inactive) and S200C/S258C (active) mutants of TmCdsA. (a) Side view along the membrane plane. Color codes: blue, S200C/S223C; orange, S200C/S258C. Stereo images are presented. **(b)** Top view along the membrane normal**.** (**c**) A zoom-in view of the engineered C223 and C258 sites in the two structures. The two cysteine residues are highlighted as sphere models. The red arrows show the slight differences between the two structures.

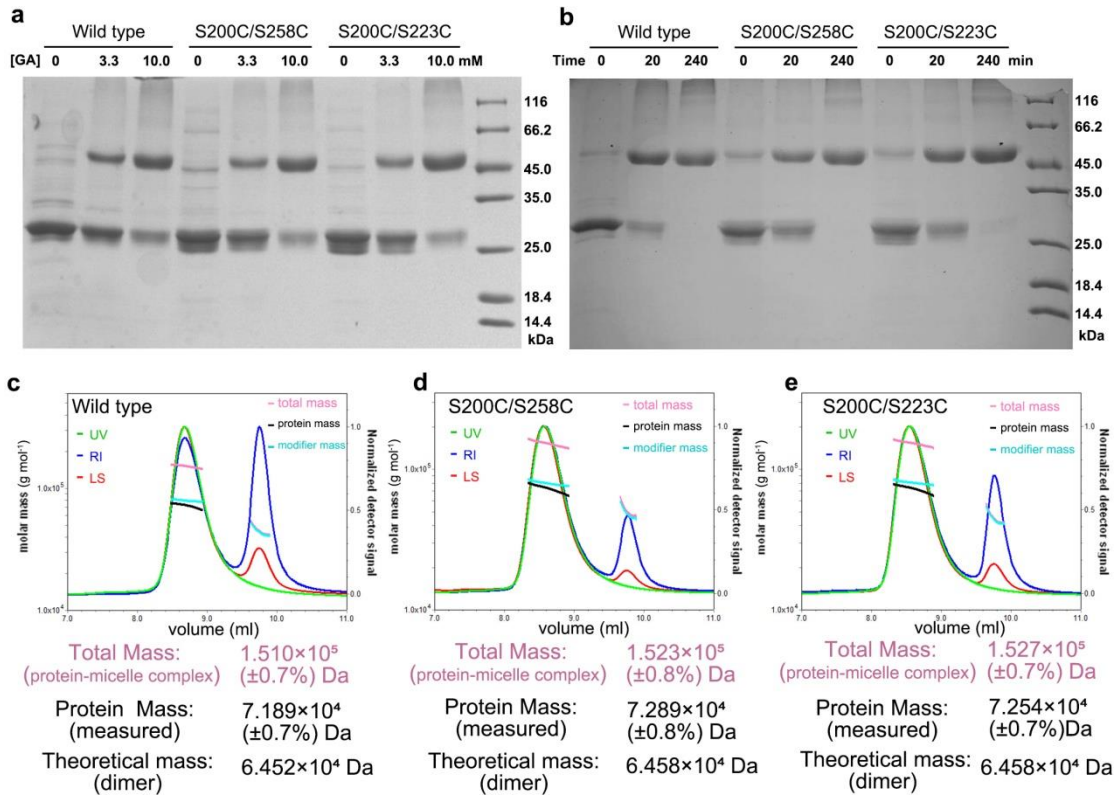

Supplementary Figure 5 | The oligomeric states of TmCdsA and mutants in solution. (a, b) Crosslinker concentration and time-dependent crosslinking kinetics of wild type TmCdsA, S200C/S258C and S200C/S223C mutants. GA, glutaraldehyde. (**c, d, e**) Size-exclusion chromatography with multi-angle light-scattering (SEC-MALS) measurements on the protein masses of wild type TmCdsA (c), S200C/S258C (d) and S200C/S223C (e) mutants.

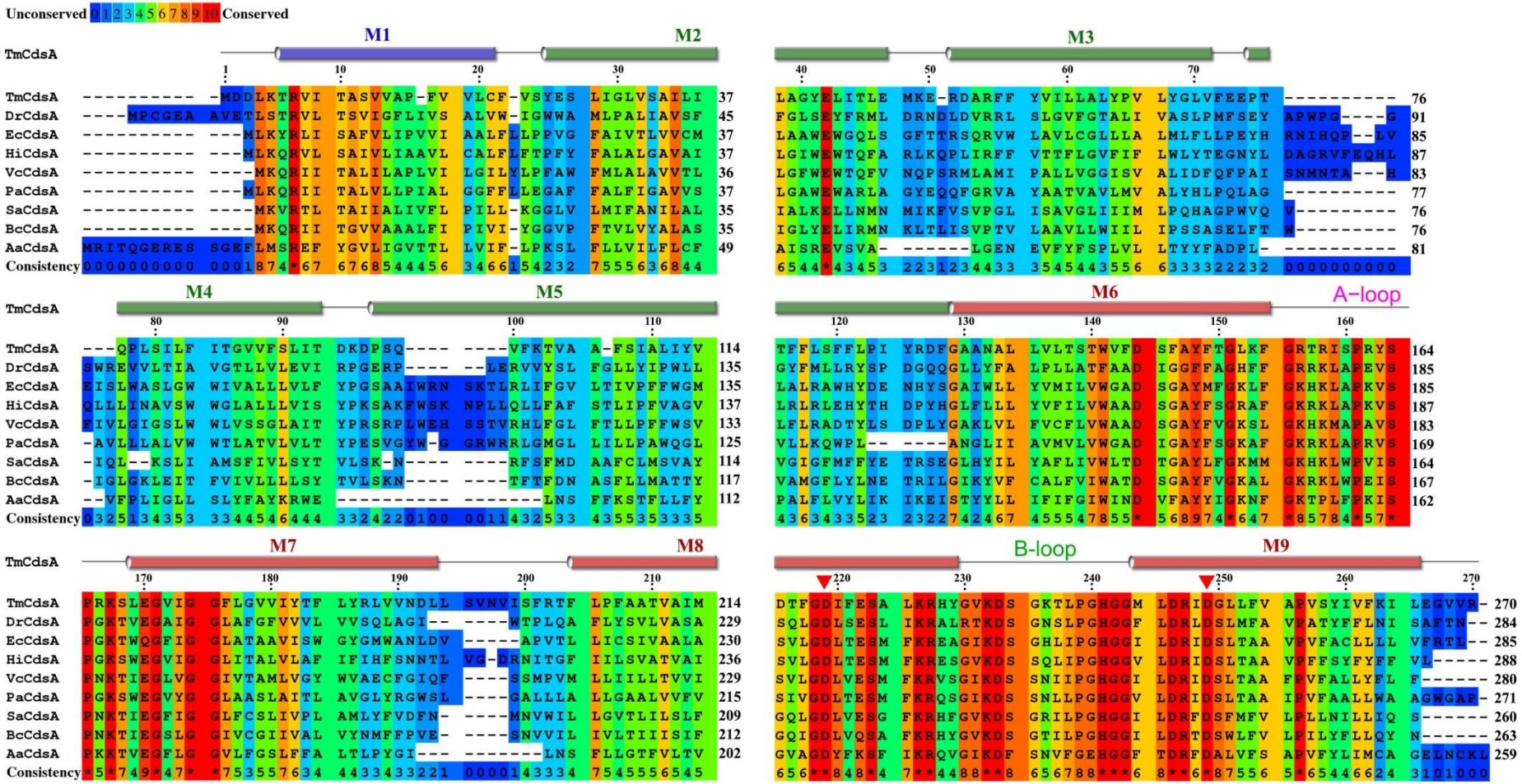
a
Unconserved 0 1 2 3 4 5 6 7 8 9 10 Conserved
M1
M2
M3
M4
M5
M6
A-loop
M7
M8
B-loop
M9
TmCdsA
DrCdsA
EcCdsA
HiCdsA
VcCdsA
PaCdsA
SaCdsA
BcCdsA
AaCdsA
Consistency

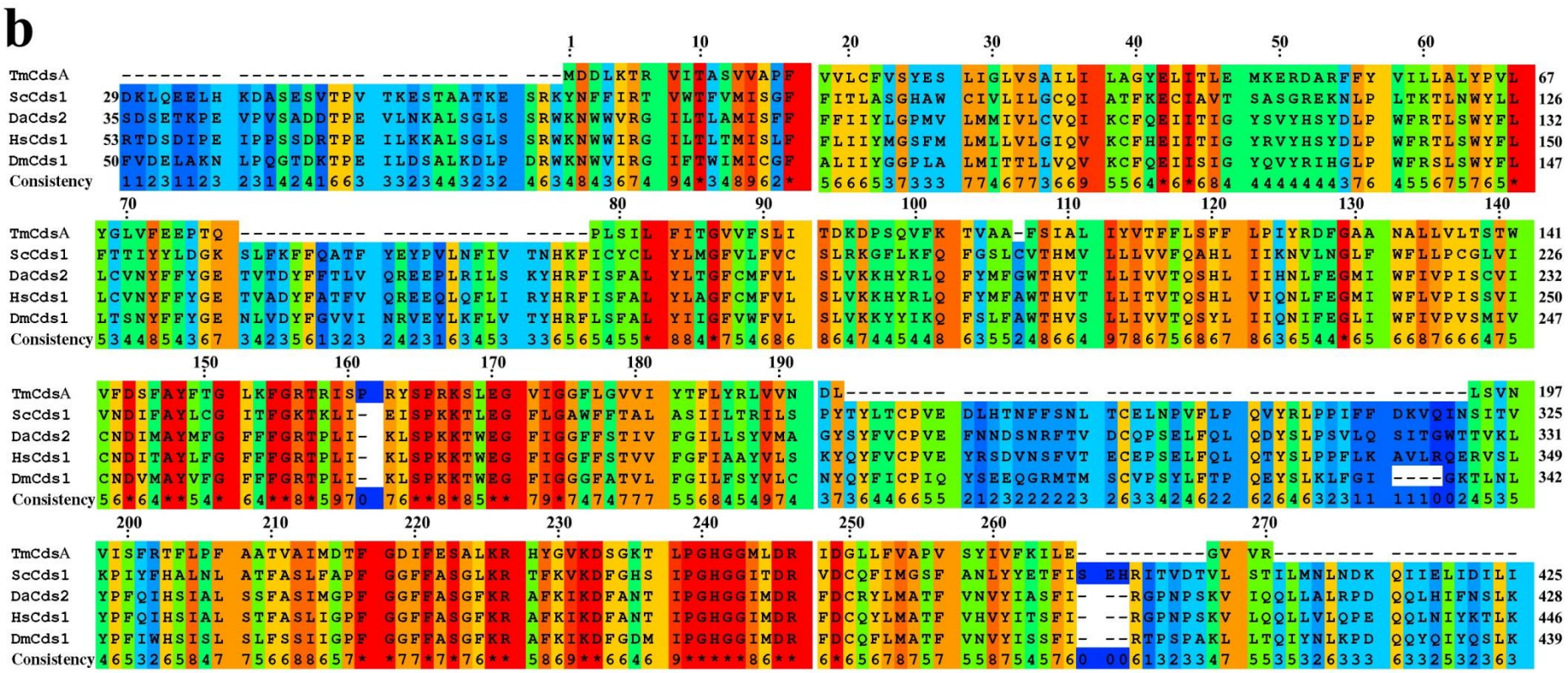

Supplementary Figure 6 | Alignment of the amino acid sequences of TmCdsA and other Cds homologs. (**a**) TmCdsA aligned with various prokaryotic Cds homologs. The different background color codes indicate the varying degree of amino acid residue conservation among the Cds homologs, with the red color highlighting identical residues and blue color denoting unconserved residues. The regions covering transmembrane M1-M9 helices are labeled above the sequence as blue, green and red cylinders. The domain-specific color codes of the transmembrane helices

are consistent with those shown in Figure 3c, namely blue for NTD, green for MD and red for CTD. The solid red triangles mark the two highly conserved Asp residues (D219 and D249) that are directly involved in binding the Mg^{2+}-K^{+} di-metal center and essential for the enzyme activity. Abbreviation of species names: Tm, *Thermotoga maritima*; Dr, *Deinococcus radiodurans*; Ec, *Escherichia coli*; Hi, *Haemophilus influenzae*; Vc, *Vibrio cholerae*; Pa, *Pseudomonas aeruginosa*; Sa, *Staphylococcus aureus*; Bc, *Bacillus cereus*; Aa, *Aquifex aeolicus*. The amino acid sequence of TmCdsA shares 27% identity or 49% similarity with that of EcCdsA which was originally purified and characterized in an early biochemical study[1]. (**b**) TmCdsA aligned with various eukaryotic Cds homologs. Sc, *Saccharomyces cerevisiae*; Da, *Danio rerio*; Hs, *Homo sapiens*; Dm, *Drosophila melanogaster*. The DmCds1 and DaCds2 are the two eukaryotic homologs reported to have essential roles in the recycling of phosphoinositide during signal transduction[2,3].

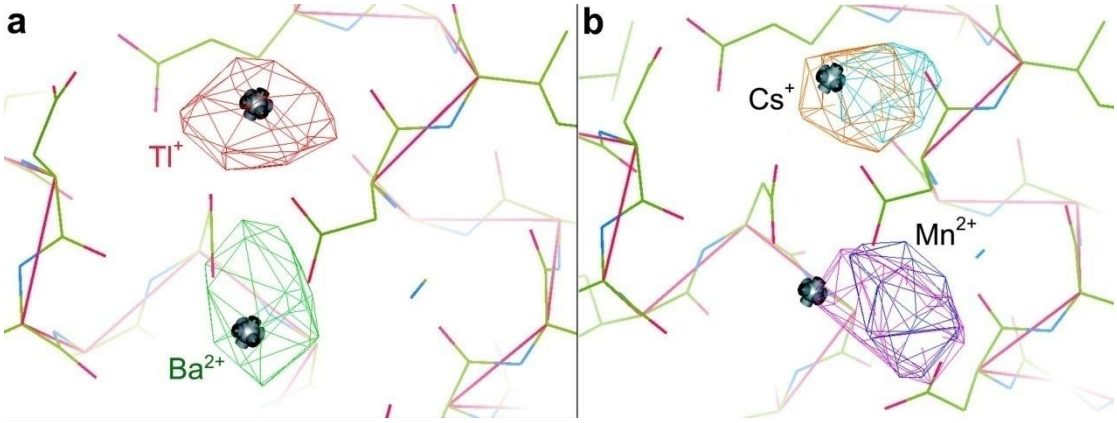

Supplementary Figure 7 | Probing the active site of TmCdsA with heavy surrogates of K^+ and Mg^{2+} ions. (a) Anomalous difference Fourier peaks of Tl^+ (red, +5.0 × σ level) and Ba^{2+} (green, +6.0 × σ level) ions bound to TmCdsA. **(b)** Isomorphous and anomalous difference Fourier peaks of Mn^{2+} and Cs^+ ion bound to TmCdsA. The F_{Mn}-F_{Mg} map in blue is contoured at +5.5 × σ level, while the Mn-anomalous difference map in purple is at +4.0 × σ level**.** The F_{Cs}-F_K map in orange and the Cs-anomalous difference map in cyan are both contoured at +6.0 × σ level.

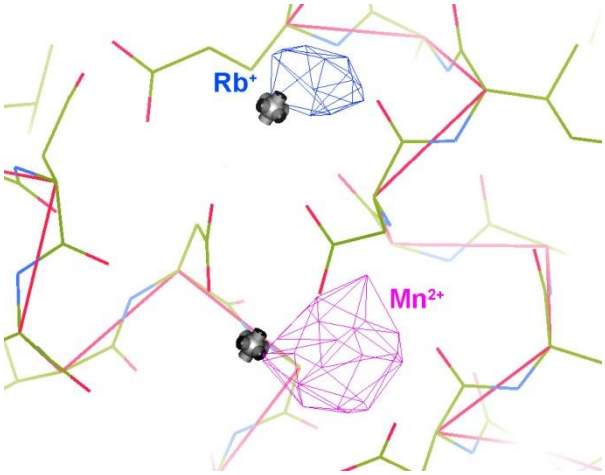

Supplementary Figure 8 | Rb^+ and Mn^{2+} ions simultaneously bind to the active site of TmCdsA. The F_{Rb+Mn}-F_{K+Mn} isomorphous difference map in blue is contoured at +3.0 × σ level. The anomalous difference map in purple using data collected at 1.54178 Å wavelength is contoured at +3.5 × σ level. Only Mn^{2+} instead of Rb^+ produces detectable anomalous signal under this wavelength**.** Both maps were computed to 4.5 Å resolution. The silver bullet models indicate the refined positions of Mg^{2+} and K^+ ions in the structure of S200C/S223C crystal. The peaks of Rb^+ and Mn^{2+} ions slightly deviate from the positions of K^+ and Mg^{2+} site due to minor changes of the unit cell dimensions in the derivatized crystal.

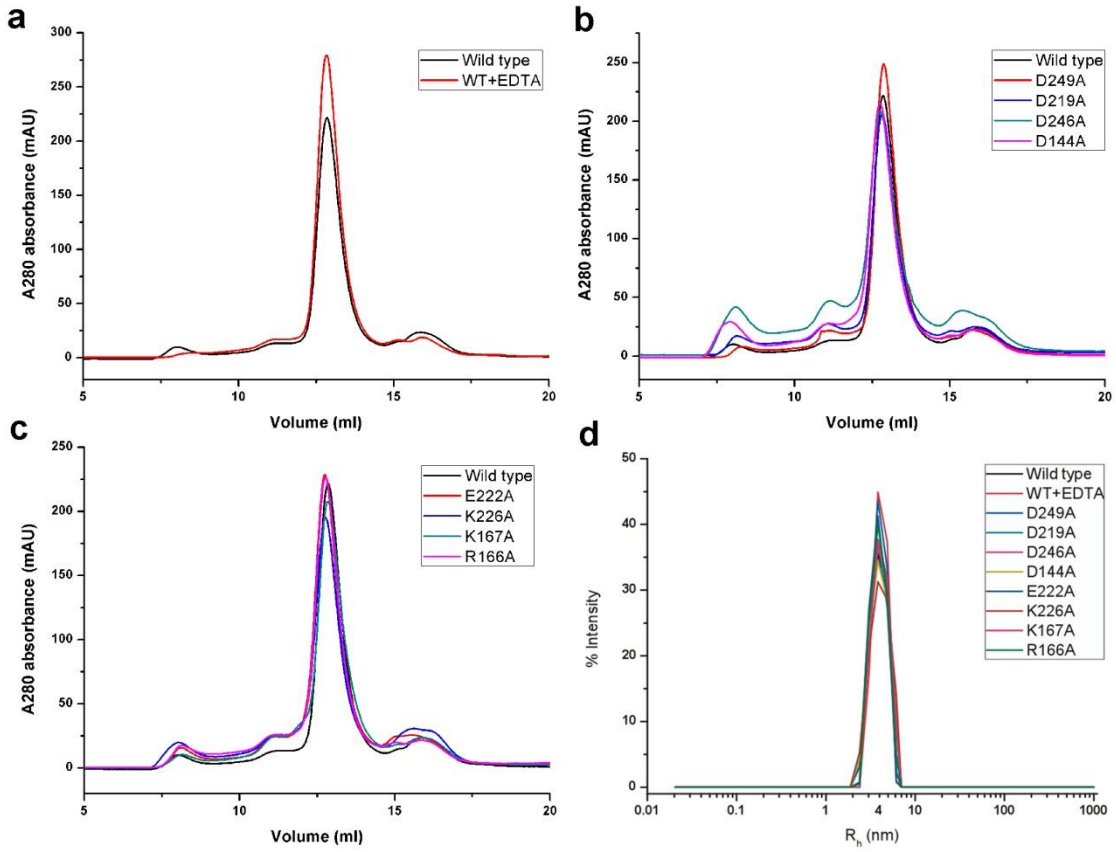

Supplementary Figure 9 | Analyses on the mono-dispersity of the wild-type, EDTA-treated TmCdsA proteins and the various mutants used for the activity assay. (**a, b and c**) Gel filtration (superdex 200 10/300 GL) profiles of the EDTA-treated TmCdsA and various mutants used for activity assay shown in Fig. 4e. For comparison, the elution profile of the wild-type protein is included in all three panels. (**d**) Dynamic light-scattering analyses on the main peak fractions (at around 12.8 ml) eluted from the gel filtration column for further verification of sample mono-dispersity. R_h (nm) represents the hydrodynamic radius of the particles in solution.

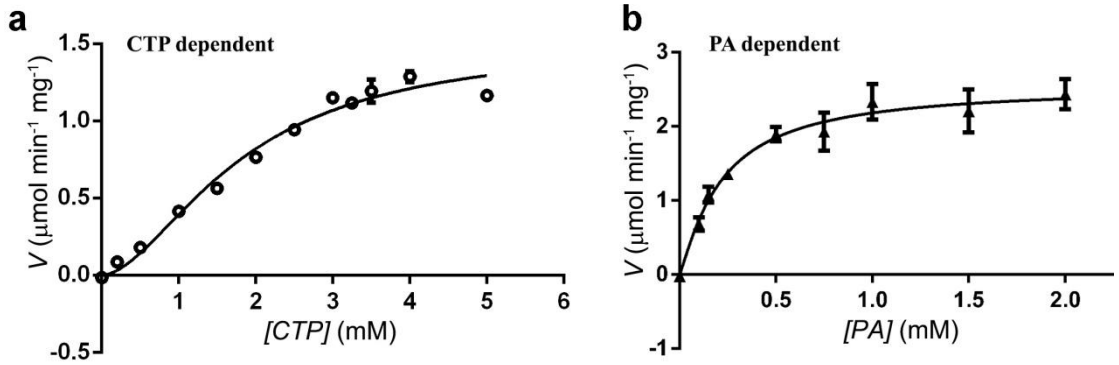

Supplementary Figure 10 | Substrate-dependent kinetic analyses of TmCdsA in the presence of 200 mM KCl and 2 mM $MgCl_2$. (**a**) CTP-dependent kinetic data measured in the presence of 2 mM DOPA. Each individual data points are plotted as mean value ± standard error (SEM as indicated by the error bars. n=4 For the data points with *[CTP]* = 0.5, 1.0, 2.0 and 3.0 mM, while the other data points were measured with n=3 instead). For those data points with small errors, the error bars are buried within the symbols. (**b**) PA-dependent kinetic data measured in the presence of 4 mM CTP. For the data points with *[PA]* = 0.75, 1 and 1.5 mM, n=4, while the others are with n=3 instead. The kinetic parameters of the fitted curves are summarized in Supplementary Table 1.

Supplementary Table 1 | Kinetic parameters of TmCdsA and EcCdsA

Enzyme	CTP Dependence			PA dependence		
	V_{max}	K_{half}/K_m [ξ]	Hill coefficient	V_{max}	K_{half}/K_m [ξ]	Hill coefficient
TmCdsA	1.52 ± 0.11	K_{half} = 1.82 ± 0.19	1.7 ± 0.2	2.55 ± 0.34	K_{half} = 0.22 ± 0.07	1.2 ± 0.4
EcCdsA[ξ]	55.0	K_m= 0.58 ± 0.16	N/A	55.0	K_m= 0.28 ± 0.05	N/A

The parameters are estimated by using the GraphPad Prism 6 software to fit the plots of initial velocity versus substrate (CTP or PA) concentration shown in Supplementary Figure 10. For CTP-dependent and PA-dependent kinetic data of TmCdsA, the allosteric sigmoidal model (($Y = V_{max}*X^h/(K_{half}{}^h + X^h)$; h = Hill coefficient) is applied for data fitting. The error presented is ± S. E. of the fit. Units for V_{max} are μmol of CDP-DAG produced per min per mg enzyme. The unit for K_{half} or K_m is mM.

[ξ] Data reported in the literature[1].

Supplementary References:

1. Sparrow, C. P. & Raetz, C. R. Purification and properties of the membrane-bound CDP-diglyceride synthetase from *Escherichia coli*. *J. Biol. Chem.* **260**, 12084-91 (1985).
2. Wu, L., Niemeyer, B., Colley, N., Socolich, M. & Zuker, C. S. Regulation of PLC-mediated signalling *in vivo* by CDP-diacylglycerol synthase. *Nature* **373**, 216-22 (1995).
3. Pan, W. et al. CDP-diacylglycerol synthetase-controlled phosphoinositide availability limits VEGFA signaling and vascular morphogenesis. *Blood* **120**, 489-498 (2012).